Journal of Magnetic Resonance 194 (2008) 147–151

Contents lists available at ScienceDirect

Journal of Magnetic Resonance

journal homepage: www.elsevier.com/locate/jmr

Communication

Interaction of anti-aggregation agent dimethylethylammonium propane sulfonate with acidic fibroblast growth factor

Long Xiang [a], Takeshi Ishii [a], Kazuo Hosoda [a], Ayumi Kamiya [a], Mayu Enomoto [a], Nobukazu Nameki [a], Yusuke Inoue [a], Kenji Kubota [a], Toshiyuki Kohno [b], Kaori Wakamatsu [a,*]

[a] Department of Chemistry and Chemical Biology, Graduate School of Engineering, Gunma University, 1-5-1 Tenjin-cho, Kiryu, Gunma 376-8515, Japan
[b] Mitsubishi Kagaku Institute of Life Sciences (MITILS), Machida, Tokyo 194-8511, Japan

ARTICLE INFO

Article history:
Received 23 January 2008
Revised 30 May 2008
Available online 20 June 2008

Keywords:
NDSB-195
Acidic FGF
Aggregation
Denaturation
Chemical shift perturbation

ABSTRACT

Prevention of aggregation is critical for analyzing protein structure. Non-detergent sulfobetaines (NDSBs) are known to prevent protein aggregation, but the molecular mechanisms of their anti-aggregation effect are poorly understood. To elucidate the underlying mechanisms, we analyzed the effects of dimethylethylammonium propane sulfonate (NDSB-195) on acidic fibroblast growth factor (aFGF). NDSB-195 (0.5 M) increased both aggregation and denaturation temperatures of aFGF by 4 °C. Chemical shift perturbation analyses indicated that many affected residues were located at the junction between a β-strand (or 3_{10}-helix) and a loop, irrespective of the chemical properties of the residue. The apparent dissociation constants of the interaction ranged from 0.04 to 3 M, indicating weak interactions between NDSB and protein molecules.

1. Introduction

Protein aggregation is one of major obstacles in protein structure analyses since it impedes crystallization [1] and results in poor resolution and low sensitivity of solution nuclear magnetic resonance (NMR) signals [2]. To prevent the aggregation of calcineurin B, Anglister et al. added CHAPS (a small zwitterionic detergent) to the sample, and observed well resolved resonances [3]. More recently, Golovanov et al. found that the equimolar mixture of glutamic acid and arginine (at 50 mM) greatly enhanced the solubility of many proteins without interfering NMR measurements by their proton resonances or disrupting intrinsic protein/RNA interactions [4]. Here, we report the application of non-detergent sulfobetaine (NDSB [5]) in NMR measurements of an unstable protein. NDSBs are a group of small compounds with a zwitterionic sulfobetaine moiety and a small hydrophobic moiety, and are known to prevent protein aggregation [5]. In fact, dimethylethylammonium propane sulfonate (NDSB-195, Fig. 1) has been successfully used to crystallize proteins [6,7]. However, the mechanisms by which NDSBs prevent protein aggregation are unclear. Thus, to explore the applicability of NDSB-195 in NMR measurements and to elucidate the stabilization mechanisms, we examined the effects of NDSB-195, by solution NMR, on human acidic fibroblast growth factor (aFGF)[1]—a protein that tends to aggregate at low ionic strengths [8].

We selected NDSB-195 from 6 commercially available NDSBs because (1) unlike NDSB-201, -256, and -256-4T, it does not contain aromatic protons which would give rise to noises in the amide proton region, (2) it is stable against UV light unlike NDSB-201 and -256-4T, (3) it has a relatively simple proton spin system unlike NDSB-221 which has a cyclohexane moiety, (4) it is relatively inexpensive compared with NDSB-211, and (5) it has been studied most extensively [5–7].

2. Results

2.1. NDSB prevents the thermal aggregation and denaturation of aFGF

Fig. 2 shows the temperature dependence of the 1D [^{15}N, ^{1}H] HSQC spectra of aFGF in the absence or presence of 0.5 M NDSB-195 (both samples contain 150 mM NaCl). In the absence of NDSB-195, signal height decreased with increasing temperature due to thermal aggregation of the protein, and the maximum height at 35 °C was less than 40% of the one at 25 °C (Fig. 2a). Conversely, in NDSB-195 presence, the height at 30 °C increased relative to that at 25 °C due to more rapid tumbling motion and the

* Corresponding author. Fax: +81 277 30 1439.
E-mail address: wakamats@chem-bio.gunma-u.ac.jp (K. Wakamatsu).

[1] *Abbreviations used:* aFGF, acidic fibroblast growth factor; CSP, chemical shift perturbation, HSQC, heteronuclear single quantum coherence; K_d, dissociation constant; NDSB, non-detergent sulfobetaine; T_a, aggregation temperature.

1090-7807/$ - see front matter © 2008 Elsevier Inc. All rights reserved.
doi:10.1016/j.jmr.2008.06.006

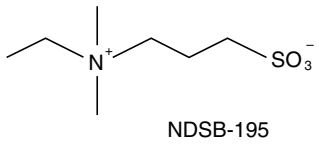

Fig. 1. Chemical structure of NDSB-195.

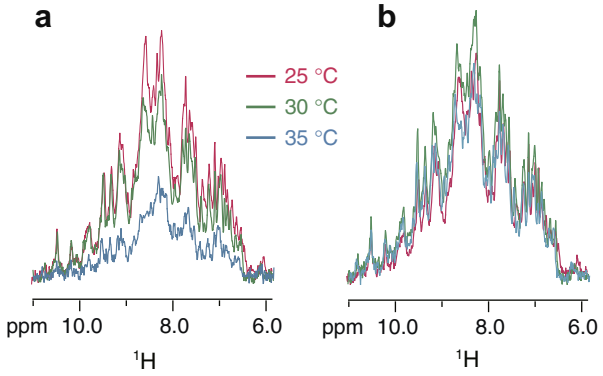

Fig. 2. Temperature dependence of the 1D-HSQC spectra of aFGF in the absence (a) or presence (b) of 0.5 M NDSB-195. Temperatures were 25 °C (magenta), 30 °C (green), and 35 °C (cyan).

intact structure of the protein molecules (Fig. 2b). Although a further temperature shift to 35 °C decreased the signal height, the maximum height retained 96% of the one at 25 °C. These observations indicate that NDSB-195 effectively prevents aFGF aggregation.

Prevention of thermal aggregation of aFGF by NDSB-195 was also demonstrated by turbidometric measurements. Fig. 3a shows the temperature dependence of sample turbidity at 350 nm. In the absence of NDSB-195, the turbidity began increasing at approximately 42 °C due to light scattering by the protein aggregates, whereas the turbidity began decreasing at 51 °C due to precipitation of the aggregates (i.e., removal from the light path). The midpoint temperature of the turbidity increase (T_a) was 45.8 °C. Inversely, the corresponding T_a value in the presence of 0.5 M NDSB-195 was 50.2 °C, and about 4 °C higher than that in its absence.

NDSB-195 also increased the denaturation temperature of aFGF. In an aFGF molecule, there exists one tryptophan residue with its side chain buried in the protein core [9]. On heating, the emission wavelength of the maximum fluorescence of aFGF shows a red shift from 302 to 330 nm (Fig. 3b) due to the exposure of the side chain in the aqueous phase. The midpoint temperature of the wavelength shifted from 48.5 °C in the absence of NDSB-195 to 52.6 °C in the presence of 0.5 M NDSB-195; an increase of 4 °C as in the case for turbidity at 350 nm.

2.2. Residues affected by NDSB-195

To determine the amino acid residues of aFGF affected by NDSB-195 and the strength of the interactions, a series of 2D HSQC spectra were recorded at increasing NDSB-195 concentrations, and the chemical shift perturbations (CSPs) on adding 0.5 M NDSB-195 are shown in Fig. 4 (CSPs at other NDSB concentrations are shown in Supplementary Figure S1). Although many residues were shifted to some extent, residues Thr48–Arg49, Gly129, and His138–Lys142 were affected more intensely than others, suggesting stronger effects of NDSB-195 on these residues. Since spatially proximate residues (<8 Å: the maximum length of NDSB-195) having similar apparent K_d values may constitute the same interaction site for NDSB, the inter-residue distance and apparent K_d values were analyzed for the affected residues, and were grouped into 11 possible interaction sites (Table 1). Although lysine and glycine residues appear frequently, acidic (Glu), neutral (Ser, Thr, and Gln), and hydrophobic (Val and Leu) residues also appear to constitute the interaction sites.

The residues listed in Table 1 are mapped along the protein sequence (Fig. 5). Interestingly, more than two-thirds of the affected residues (13 of 19) are located in the junction between a secondary structure (β-strand or 3_{10}-helix) and a loop. The residues in Table 1 are mapped on the tertiary structure of aFGF [10] (Fig. 6). Residues exhibiting large shift changes were also mapped, although their apparent K_d values could not be determined reliably: His93,

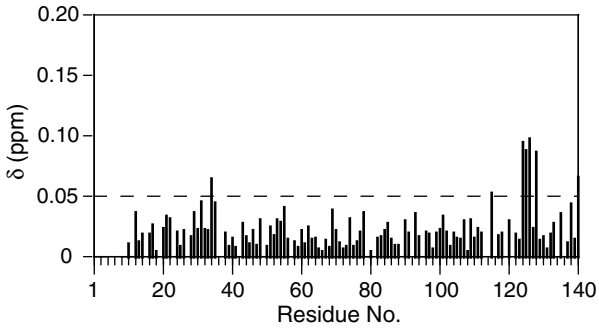

Fig. 4. CSP ($\Delta\delta$) of aFGF on addition of 0.5 M NDSB-195 as a function of the residue number.

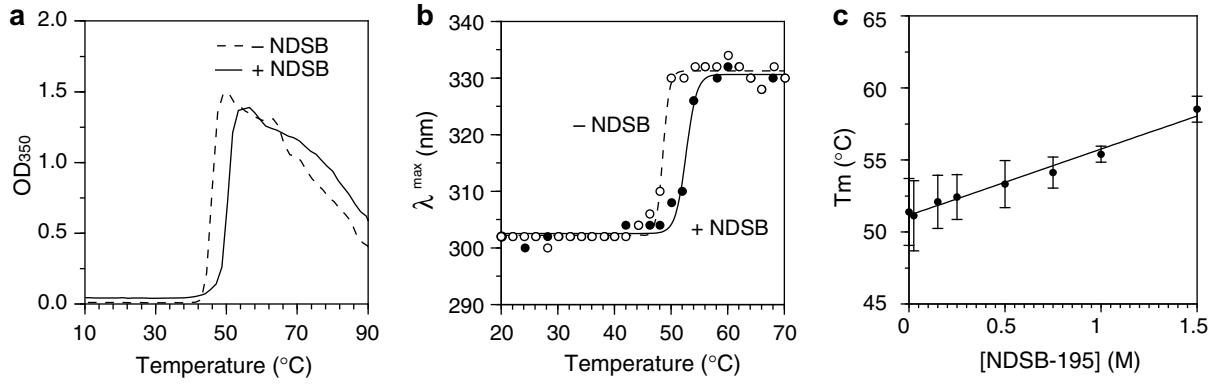

Fig. 3. Effects of NDSB-195 on the thermal stability of aFGF. (a) Turbidity at 350 nm as a function of temperature in the absence (broken line) and presence of 0.5 M NDSB-195 (solid line). (b) The maximum fluorescence emission wavelength as a function of temperature in the absence (broken line) and presence of 0.5 M NDSB-195 (solid line). Excitation wavelength, 280 nm. (c) NDSB-195 concentration dependence of the aggregation temperature (T_a). Bars represent SEMs of three independent experiments.

Table 1
NDSB-interaction sites in aFGF and their apparent dissociation constants

Apparent K_d (M)	Site number	Residues
~0.04	1	G140, K142
0.1–0.5	2	K114, K115
	3	K132
0.5–1.0	4	G43
	5	Q57
1.0–3.0	6	S31, G34
	7	T48, R49, G129
	8	G66, V68
	9	G76
	10	E105, L147
	11	L149, S152

The underlined residues are located in the junction between a β-strand (or 3_{10}-helix) and a loop.

Tyr107, Tyr139, and Asp154. Such affected residues are widely distributed throughout the structure.

3. Discussion

3.1. NDSB-interaction sites on aFGF

We analyzed the interaction of NDSB with aFGF by solution NMR analysis. Although in some cases, NDSB-195 molecules are observed in the crystal structure of proteins crystallized in the presence of this additive [6,7], such observations are rather rare since only sites with high affinities are determined by this method [6,11]. Since solution NMR analysis can detect weak molecular interactions, it is appropriate for the analyses of NDSB–protein interactions. We identified 19 residues with an apparent K_d value of <3 M whose chemical shifts appeared affected. Because the CSP of a residue does not necessarily indicate its direct interaction with NDSB-195, we grouped the spatially close residues with similar K_d values to find the possible interaction sites (Table 1). NDSB-195 exhibits an obvious weak preference for particular chemical structures of protein residues. This may be since NDSB-195 possesses all of the basic, acidic, and hydrophobic moieties in one molecule, which enables ionic and hydrophobic interactions as well as hydrogen bonding. In fact, in the crystal structure of purine nucleoside kinase, the NDSB-195 molecule was in close proximity to residues with different chemical properties (valine, glycine, serine, arginine, etc.) [6]. More than two-thirds of the affected residues are located in the junction between a secondary structure and a loop (Fig. 5), and most interaction sites contain such residues in the junction (Table 1). The observation that glycine residues are affected by NDSB-195 more frequently than other residues may be due to the frequent occurrence of this residue in loops [12] and to the flexibility of this residue (larger susceptibility to conformational perturbations). Acidic FGF contains a β-trefoil motif with a 3-fold symmetry axis [9]. The distribution of the interaction sites, however, does not demonstrate 3-fold symmetry (Fig. 6).

3.2. Comparison of NDSB-195 with heparin analogs

For its biological activities, aFGF requires the association with heparin, and heparin and its analogs are known to stabilize aFGF [13]. Heparin binds to the C-terminal region of aFGF, and the binding sites have been analyzed in detail, using heparin analogs that

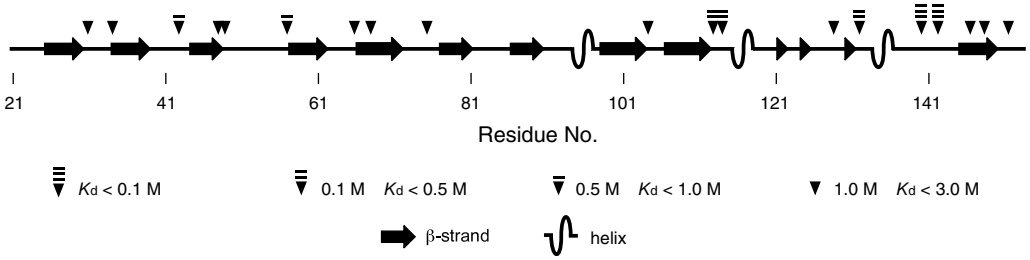

Fig. 5. The residues whose chemical shifts were affected by NDSB-195 with apparent K_d values smaller than 3 M are indicated along the sequence of aFGF. Different affinities of the interaction are indicated by different symbols.

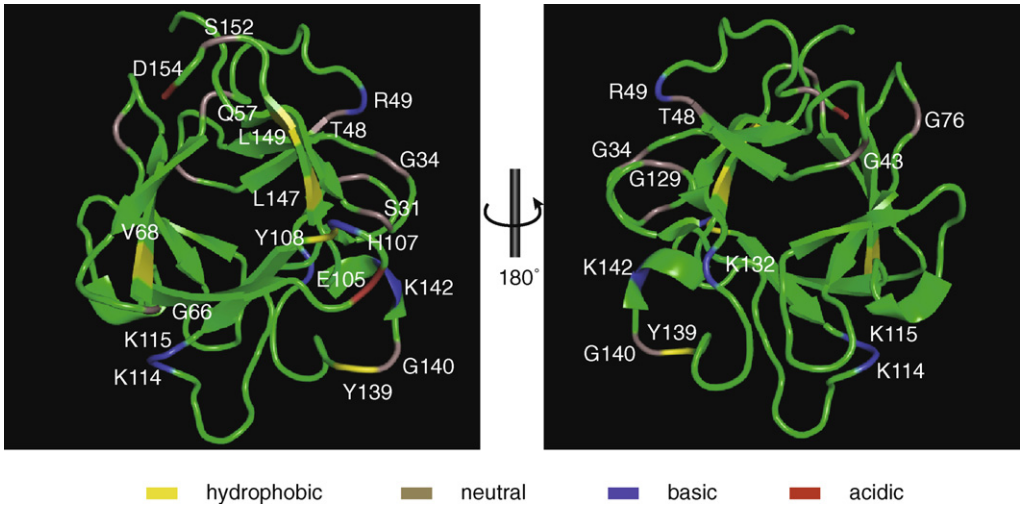

Fig. 6. NDSB-interaction sites are mapped on the tertiary structure of aFGF (PDB ID: 2ERM [10]).

do not induce protein oligomerization [13]. Eleven residues—Phe122, Asn128, Cys131, Lys132, Arg133, Gly134, Thr137, His138, Tyr139, Lys142, and Ala143—exhibited large ($\Delta\delta > 0.15$) CSPs with Lys132 being the largest ($\Delta\delta > 0.9$) on addition of sucrose octasulfate (SOS) [13]. CSPs were also observed at the C-terminal region on adding NDSB-195 (Fig. 4). The residues exhibiting CSPs—Gly129, His138, Tyr139, Gly140, and Lys142—differ, however, from those in the case of SOS, and the perturbation value did not exceed 0.10 for any residues (Fig. 4). Because two residues in this region—Gly140 and Lys142—exhibited the highest affinity to NDSB-195 (~0.04 M), we investigated whether this high-affinity interaction between NDSB-195 and aFGF had a greater impact on the protein stabilization than the interaction with other residues. The aggregation temperature (T_a) increased almost linearly with the NDSB-195 concentration (Fig. 3c). This observation excludes the possibility of the larger impact of the interaction of NDSB-195 with Gly140 and Lys142. Since the affinities are widely distributed in the range of 0.04–3.0 M (Table 1), Fig. 3c suggests that the interaction of each site with NDSB-195 contributes fairly equally to the protein stabilization.

3.3. Possible Hofmeister effect of NDSB-195

Because NDSBs contain a sulfonate group, the stabilization by NDSB might be ascribed to their Hofmeister effect as observed for sulfate ions [14]. Direct comparison of the stabilizing effects of NDSB-195 and sulfate ions is difficult, however, because sulfate ions strongly stabilize aFGF at a low concentration (0.1 M) [8]. This particular stabilizing effect of sulfate ions on aFGF may be ascribed to the direct specific binding of sulfate ions to the heparin-binding site on aFGF rather than to the Hofmeister effect. It is because the Hofmeister effect requires high concentration (0.2–1 M) of salts [15]. On the other hand, the stabilization by NDSB-195 is not ascribed to the specific binding to the sulfate/heparin-binding site(s) on aFGF as described in the previous section. The elucidation of the protein stabilizing mechanisms of NDSB-195 will require further analyses.

3.4. Stabilization of other proteins by NDSB-195

NDSB-195 increased the aggregation temperature of G protein α subunit, γ-globulins, and even ubiquitin (Ishii et al., to be published) as well as aFGF. NDSB-195's preference for particular amino acid types was found to be rather weak, and NDSB-195 was found to affect the residues in secondary structure/loop junctions. Although the mechanisms whereby NDSBs prevent protein aggregation are still elusive, it is possible that NDSB-195 stabilizes many proteins since most proteins have such junctions.

3.5. Application of NDSB-195 to NMR measurements

NDSB-195 may be beneficial for stabilizing protein samples used for heteronuclear solution NMR measurements. NDSB-195 (0.5 M) prevented signal loss due to thermal precipitation (Fig. 2) with no increase in pulse width and a negligible increase in sample viscosity (data not shown). The absence of pulse length increase by the addition of 0.5 M NDSB-195 is quite beneficial because the addition of regular salts such as sodium chloride and ammonium sulfate results in the longer pulse length, lower sensitivity, more sample heating, and sometimes prohibition of using cryogenic probes with high sensitivity. The distortion in water resonance, which would lower the sensitivity, was not observed at all (data not shown). No precipitate was observed in the aFGF sample containing 0.5 M NDSB (and 0.15 M NaCl) at 20 °C for 1 month, while in the presence of 0.15 M NaCl alone, the sample exhibited considerable precipitation (data not shown).

We recommend trying 0.5 M NDSB-195 at first to unstable protein samples. When this concentration of NDSB is effective but not satisfactory, we increase the concentration up to 1 M. When 0.5 M NDSB-195 exhibits satisfactory stabilization, we may try lower concentrations to decrease noises in ^{13}C–^{1}H planes and to increase receiver gain.

The very limited perturbation in chemical shifts for amide resonances ($\Delta\delta < 0.1$ at 0.5 M) and for methly resonances (Supplementary Figure S2) suggests that protein structure is not perturbed significantly upon adding NDSB-195. The weak protein–NDSB-195 interactions ($K_d > 10^{-2}$ M) preclude the possible inhibition of enzymatic activities and physiological protein–protein interactions in the presence of NDSB-195 since the affinity between enzymes and substrates is stronger than protein–NDSB-195 interactions by two orders of magnitude. In fact, NDSB did not exhibit significant inhibitory effects on enzyme activities (*E. coli* β-galactosidase and yeast ubiquitin hydrolase) and protein–protein interactions (activation of G protein by muscarinic acetylcholine receptor) as far as we examined (Ishii et al., to be published). Furthermore, NDSB-195 did not significantly affect transverse relaxation rates (R_2) of amide protons of aFGF (Xian et al., to be published).

4. Experimental

4.1. Preparation of aFGF

The gene encoding human aFGF [16] was cloned from the total mRNA of human hepatoblastoma cells HepG2 by reverse transcription-polymerase chain reaction (RT-PCR); its open reading frame was ligated into the NdeI/XhoI sites of the pET20b vector (Novagen), which possesses a hexahistidine tag at the C-terminus of the protein. Uniformly ^{15}N-labeled aFGF ([u-^{15}N] aFGF) was expressed and purified as described [8] and concentrated in buffer A (25 mM sodium phosphate, pH 6.6, 150 mM NaCl) by ultrafiltration using Amicon Ultra-5 (Millipore) at 4 °C.

4.2. Thermal aggregation and denaturation

The thermal aggregation profile of aFGF (5 μM in buffer A) was recorded on a Shimadzu UV-2550 UV–VIS spectrophotometer equipped with a TMSPC-8 temperature controller. The turbidity was monitored at 350 nm from 10 to 90 °C at a heating rate of 0.5 °C/min. The thermal denaturation profile of aFGF (1 μM in buffer A) was recorded on a JASCO FP-6500 spectrofluorometer. Emission spectra (300–600 nm, excitation at 280 nm) were obtained for the temperature range of 20–70 °C at 2-°C intervals with 20-s equilibration time at each temperature point and a heating rate of 2 °C/min.

4.3. NMR measurements

All NMR spectra were recorded on Bruker ARX 400 spectrometer at 400 MHz for protons. [u-^{15}N] aFGF (0.4 mM) was diluted in buffer A supplemented with 0.5 mM 1,4-dioxane for chemical shift referencing [17] and 10% D_2O. NDSB-195 stock solution (3 M) was prepared by dissolving NDSB-195 in the same buffer followed by filtration through a 0.2-μm filter. At 25, 30, and 35 °C, 1D [^{1}H-^{15}N] HSQC spectra were recorded. To analyze the effects of NDSB-195 on aFGF, a series of 2D ^{1}H-^{15}N HSQC spectra of 0.4 mM [u-^{15}N] aFGF were recorded in the presence of 0, 37, 108, 240, 333, 420, 500, 736, and 1,000 mM NDSB-195 at 20 °C, with 1,024 and 256 complex data points at t_2 and t_1, respectively, and 16 scans per t_1 increment. CSP of each HSQC resonance ($\Delta\delta$) was calculated:

$$\Delta\delta = \sqrt{(0.2 \times \Delta\delta_N)^2 + \Delta\delta_H^2} \quad (1)$$

$\Delta\delta_N$ and $\Delta\delta_H$ indicate the chemical shift changes (in ppm) of amide nitrogen and proton, respectively [13]. Apparent dissociation constants (K_d) were estimated for each residue [18]. We ignored residues exhibiting poor correlation ($r^2 < 0.5$) or a very high apparent K_d value (>3 M). Data processing was performed using NMRPipe software [19]. All ^1H–^{15}N HSQC signals were assigned based on the published assignments of aFGF [8] and confirmed by referring to the ^{15}N-edited NOESY-HSQC spectrum. The numbering of residues adopted in this study corresponds to that used in Ref. [10] and is larger by 14 as compared to those adopted in refs. [8 and 20].

Acknowledgments

We thank Prof. Kenji Osawa and Dr. Fumio Hayashi for permitting the use of the spectrofluorometer; Prof. Hiroaki Sawai and Dr. Hiroaki Ozaki, for permitting the use of the spectrophotometer; and Dr. Yasuko Iizuka, for her helpful discussions and encouragement.

Appendix A. Supplementary data

Supplementary data associated with this article can be found, in the online version, at doi:10.1016/j.jmr.2008.06.006.

References

[1] W.W. Wilson, Monitoring crystallization experiments using dynamic light scattering: assaying and monitoring protein crystallization in solution, Methods 1 (1990) 110–117.
[2] S. Bagby, K.I. Tong, M. Ikura, Optimization of protein solubility and stability for protein nuclear magnetic resonance, Methods Enzymol. 339 (2001) 20–41.
[3] J. Anglister, S. Grzesiek, H. Ren, C.B. Klee, A. Bax, Isotope-edited multidimensional NMR of calcineurin B in the presence of the non-deuterated detergent CHAPS, J. Biomol. NMR 3 (1993) 121–126.
[4] A.P. Golovanov, G.M. Hautbergue, S.A. Wilson, L.-Y. Lian, A simple method for improving protein solubility and long-term stability, J. Am. Chem. Soc. 126 (2004) 8933–8939.
[5] L. Vuillard, C. Braun-Breton, T. Rabilloud, Non-detergent sulphobetaines: a new class of mild solubilization agents for protein purification, Biochem. J. 305 (1995) 337–343.
[6] H.D. Pereira, G.R. Franco, A. Cleasby, R.C. Garratt, Structures for the potential drug target purine nucleoside phosphorylase from *Schistosoma mansoni* causal agent of schistosomiasis, J. Mol. Biol. 353 (2005) 584–599.
[7] C.A. Brautigam, B.S. Smith, Z. Ma, M. Palnitkar, D.R. Tomchick, M. Machius, J. Deisenhofer, Structure of the photolyase-like domain of cryptochrome 1 from *Arabidopsis thaliana*, Proc. Natl. Acad. Sci. USA 101 (2004) 12142–12147.
[8] K. Ogura et al., Solution structure of human acidic fibroblast growth factor and interaction with heparin-derived hexasaccharide, J. Biomol. NMR 13 (1999) 11–24.
[9] X. Zhu, H. Komiya, A. Chirino, S. Faham, G.M. Fox, T. Arakawa, B.T. Hsu, D.C. Rees, Three-dimensional structures of acidic and basic fibroblast growth factors, Science 251 (1991) 90–93.
[10] A. Canales et al., activated by a hexasaccharide heparin-analogue, FEBS J. 273 (2006) 4716–4727.
[11] L. Vuillard, B. Baalbaki, M. Lehmann, S. Nørager, P. Legrand, M. Roth, Protein crystallography with non-detergent sulfobetaines, J. Cryst. Growth 168 (1996) 150–154.
[12] S.A. Showalter, K.B. Hall, Altering the RNA-binding mode of the U1A RBD1 protein, J. Mol. Biol. 335 (2004) 465–480.
[13] Y. Chi, T.K. Kumar, I.M. Chiu, C. Yu, ^{15}N NMR relaxation studies of free and ligand-bound human acidic fibroblast growth factor, J. Biol. Chem. 275 (2000) 39444–39450.
[14] P.H. von Hippel, K.Y. Wong, Neutral salts: the generality of their effects on the stability of macromolecular conformations, Science 145 (1964) 577–580.
[15] C.H. Ramos, R.L. Baldwin, Sulfate anion stabilization of native ribonuclease A both by anion binding and by the Hofmeister effect, Protein Sci. 11 (2002) 1771–1778.
[16] R.L. Strausberg et al., Generation and initial analysis of more than 15,000 full-length human and mouse cDNA sequences, Proc. Natl. Acad. Sci. USA 99 (2002) 16899–16903.
[17] A. Shimizu, M. Ikeguchi, S. Sugai, Appropriateness of DSS and TSP as internal references for 1H NMR studies of molten globule proteins in aqueous media, J. Biomol. NMR 4 (1994) 859–862.
[18] S.A. Lee, R. Eyeson, M.L. Cheever, J. Geng, V.V. Verkhusha, C. Burd, M. Overduin, T.G. Kutateladze, Targeting of the FYVE domain to endosomal membranes is regulated by a histidine switch, Proc. Natl. Acad. Sci. USA 102 (2005) 13052–13057.
[19] F. Delaglio, S. Grzesiek, G.W. Vuister, G. Zhu, J. Pfeifer, A. Bax, NMRPipe: a multidimensional spectral processing system based on UNIX pipes, J. Biomol. NMR 6 (1995) 277–293.
[20] S.R. Brych, S.I. Blaber, T.M. Logan, M. Blaber, Structure and stability effects of mutations designed to increase the primary sequence symmetry within the core region of a β-trefoil, Protein Sci. 10 (2001) 2587–2599.